Natural convection flow of a couple stress fluid between two vertical parallel plates with Hall and ion-slip effects

Article *in* Acta Mechanica Sinica · October 2012

DOI: 10.1007/s10409-011-0523-z

CITATIONS
13

READS
147

2 authors, including:

D. Srinivasacharya
National Institute of Technology, Warangal
219 PUBLICATIONS **3,185** CITATIONS

SEE PROFILE

Acta Mech. Sin. (2012) 28(1):41–50
DOI 10.1007/s10409-011-0523-z

RESEARCH PAPER

Natural convection flow of a couple stress fluid between two vertical parallel plates with Hall and ion-slip effects

D. Srinivasacharya · K. Kaladhar

Received: 12 May 2011 / Revised: 22 June 2011 / Accepted: 29 August 2011

Abstract The Hall and ion-slip effects on fully developed electrically conducting couple stress fluid flow between vertical parallel plates in the presence of a temperature dependent heat source are investigated. The governing non-linear partial differential equations are transformed into a system of ordinary differential equations using similarity transformations. The resulting equations are then solved using the homotopy analysis method (HAM). The effects of the magnetic parameter, Hall parameter, ion-slip parameter and couple stress fluid parameter on velocity and temperature are discussed and shown graphically.

Keywords Free convection · Couple stress fluid · Magnetohydrodynamics · Hall and ion-slip effects · HAM

1 Introduction

Natural convection heat transfer and fluid flow in vertical parallel plate channels have been the focus of extensive investigation for many decades due to their wide range of heat exchange applications such as cooling of electronic equipment, solar collectors and passive solar heating, ventilation of buildings and heat removal in nuclear technology application. Studies on laminar natural convection between vertical parallel plates date back to 1942 when Elenbaas [1] did experimental and theoretical analysis on natural convection between isothermal parallel plates and presented an optimization of heat transfer rate. Bodoia and Osterle [2] numerically analyzed the development of free convection boundary layer between parallel isothermal vertical plates for the case of symmetric heating using finite difference method and obtained results of variation in temperature, pressure and velocity throughout the flow field. Aung et al. [3] conducted experimental and numerical studies on the evolution of laminar free convection between vertical flat plates with asymmetric heating, under the thermal boundary conditions of uniform heat flux and uniform wall temperature. Since then a number of studies have been reported in the literature with focus concentrated on the problem of free convection heat transfer and fluid flow between vertical parallel plates.

In recent years, several convection heat transfer and fluid flow problems have received new attention within the more general context of magnetohydrodynamics (MHD). Several investigators have extended many of the available convection heat transfer and fluid flow problems to include the effects of magnetic fields for those cases when the fluid is electrically conducting. Free convective flow of a viscous, incompressible, electrically conducting fluid through a porous medium between two vertical parallel plates which are heated or cooled uniformly, under a pressure gradient in the presence of a uniform transverse magnetic field has been studied by Singh [4]. Singha and Deka [5] have considered the unsteady viscous incompressible free convection flow of an electrically conducting fluid between two heated vertical parallel plates in the presence of a uniform magnetic field applied transversely to the flow. A two dimensional steady laminar free convective flow of viscous incompressible fluid between two parallel porous walls was considered by Omowaye and Koriko [6]. In most of the MHD flow problems, the Hall and ion-slip terms in Ohms law were ignored. However, in the presence of strong magnetic field, the influence of Hall current and ion-slip are important. Tani [7] studied the Hall effects on the steady motion of electrically conducting viscous fluid in channels. Hall and ion-slip effects on MHD Couette flow with heat transfer have been considered by Soundelgekar et al. [8]. Attia [9] consid-

D. Srinivasacharya (✉) · K. Kaladhar
Department of Mathematics
National Institute of Technology
Warangal-506004, India
e-mail: dsc@nitw.ac.in; dsrinivasacharya@yahoo.com

ered the steady Couette flow of an electrically conducting viscous incompressible fluid between two parallel horizontal non-conducting porous plates with heat transfer, taking the ion-slip into consideration.

During recent years the study of convection heat and mass transfer in non-Newtonian fluids has received much attention and this is because the traditional Newtonian fluids can not precisely describe the characteristics of the real fluids. Ziabakhsh and Domairry [10] have obtained the solution for natural convection of the Rivlin–Ericksen fluid of grade three between two infinite parallel vertical flat plates. Sajid et al. [11] studied fully developed mixed convection flow of a viscoelastic fluid between permeable parallel vertical walls using HAM. In addition, progress has been considerably made in the study of heat and mass transfer in magneto hydrodynamic flow of non-Newtonian fluids for the purpose of facilitating its application to many devices, like the MHD power generator, aerodynamics heating, electrostatic precipitation and Hall accelerator etc. Different models have been proposed to explain the behavior of non-Newtonian fluids. Among these, couple stress fluids introduced by Stokes [12] have distinct features, such as the presence of couple stresses, body couples and non-symmetric stress tensor. The couple stress fluid theory presents models for fluids whose microstructure is of mechanical significance. The effect of very small microstructure in a fluid can be felt if the characteristic geometric dimension of the problem considered is of the same order of magnitude as the size of the microstructure. The main feature of couple stresses is to introduce a size dependent effect. Classical continuum mechanics neglects the size effect of material particles within the continua. This is consistent with ignoring the rotational interaction among particles, which results in symmetry of the force-stress tensor. However, in some important cases such as fluid flow with suspended particles, this can not be true and a size dependent couple-stress theory is needed. The spin field due to microrotation of freely suspended particles set up an antisymetric stress, known as couple-stress, leading thus to couple-stress fluid. These fluids are capable of describing various types of lubricants, blood, suspension fluids etc. The study of couple-stress fluids has applications in a number of processes that occur in various industries such as the extrusion of polymer fluids, solidification of liquid crystals, cooling of metallic plate in a bath, and colloidal solutions etc. Stokes [12] discussed the hydromagnetic steady flow of a fluid with couple stress effects. A review of couple stress (polar) fluid dynamics was reported by Stokes [13]. Srinivasacharya and Srikanth [14] studied the effect of couple stresses on the flow in a constricted annulus.

The homotopy analysis method [15], first proposed by Liao in 1992, is one of the most efficient methods in solving different types of nonlinear equations such as coupled, decoupled, homogeneous and non-homogeneous. Also, HAM provides us with a great freedom to choose different base functions to express the solution of a nonlinear problem [16]. The application of HAM in engineering problems is extensively considered by scientists, because HAM provides us with a convenient way to control the convergence of approximation series, which depicts a fundamental qualitative difference in analysis between HAM and other methods. Later Liao [17] presented an optimal homotopy analysis approach for strongly nonlinear differential equations. HAM is used to get analytic approximate solutions for heat transfer of a micropolar fluid through a porous medium with radiation by Rashidi [18]. Si et al. [19] derived HAM solutions for the asymmetric laminar flow in a porous channel with expanding or contracting walls. Recent developments of HAM, like convergence of HAM solution, Optimality of convergence control parameter were discussed by Turkyilmazoglu [20,21].

In this paper, we have investigated the Hall and ion-slip effects on the steady free convective heat transfer flow of couple stress fluid between two vertical parallel plates. The Homotopy Analysis method is employed to solve the governing nonlinear equations. Convergence of the derived series solution is analyzed, and the behavior of emerging flow parameters on the velocity and temperature is discussed.

2 Mathematical formulation

Consider an incompressible electrically conducting couple stress fluid flow between two vertical parallel plates at distance $2d$ apart. Choose the coordinate system such that x-axis be taken along vertically upward direction through the central line of the channel, y is perpendicular to the plates and the two plates are infinitely extended in the direction of x and z. The plates of the channel are at $y = \pm d$. The flow is subjected to a uniform magnetic field perpendicular to the flow direction with the Hall and ion-slip effects. Since the effect of Hall and ion-slip current gives rise to forces in the z-direction, which induces a cross flow in that direction and hence the flow becomes three dimensional. Assume that the flow is steady and the magnetic Reynolds number is very small so that the induced magnetic field can be neglected in comparison with the applied magnetic field. Further, assume that all the fluid properties are constant except the density in the buoyancy term of the momentum equation. The flow configuration and the coordinates system are shown in Fig. 1.

With the above assumptions, the equations governing the steady flow of an incompressible couple stress fluid, under usual MHD approximations are

$$\frac{\partial v}{\partial y} = 0, \tag{1}$$

$$\rho v \frac{\partial u}{\partial y} = \mu \frac{\partial^2 u}{\partial y^2} - \eta_1 \frac{\partial^4 u}{\partial y^4} + \rho g \beta_T (T - T_0) - \frac{\sigma B_0^2}{\alpha_e^2 + \beta_h^2}(\alpha_e u + \beta_h w), \tag{2}$$

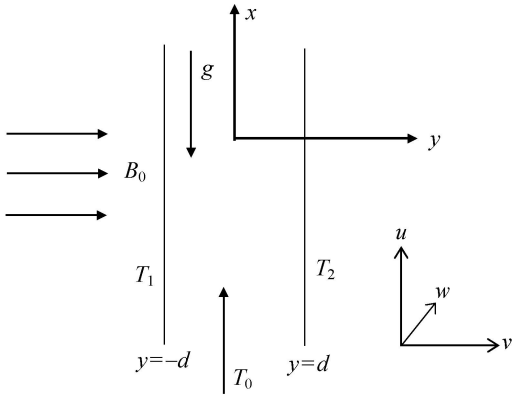

Fig. 1 Physical model and coordinate system

$$\rho v\frac{\partial w}{\partial y} = \mu\frac{\partial^2 w}{\partial y^2} - \eta_1\frac{\partial^4 w}{\partial y^4} + \frac{\sigma B_0^2}{\alpha_e^2+\beta_h^2}(\beta_h u - \alpha_e w), \tag{3}$$

$$\rho C_p v\frac{\partial T}{\partial y} = K_f\frac{\partial^2 T}{\partial y^2} + 2\mu\left[\left(\frac{\partial u}{\partial y}\right)^2 + \left(\frac{\partial w}{\partial y}\right)^2\right] + \eta_1\left[\left(\frac{\partial^2 u}{\partial y^2}\right)^2 + \left(\frac{\partial^2 w}{\partial y^2}\right)^2\right] + \gamma_0 v(T - T_0), \tag{4}$$

where u, v, w are, respectively, the x-, y- and z-components of the velocity, ρ is the density, g is the acceleration due to gravity, C_p is the specific heat, μ is the coefficient of viscosity, β_h is the Hall parameter, β_i is the ion-slip parameter, $\alpha_e = 1 + \beta_h\beta_i$, β_T is the coefficient of thermal expansion, K_f is the coefficient of thermal conductivity, η_1 is the additional viscosity coefficient which specifies the character of couple-stresses in the fluid. T_0 is the temperature in hydrostatic state, γ_0 is the constant of proportionality and $\gamma_0 v(T - T_0)$ is the amount of heat generated per unit volume in unit time, which is assumed to be a linear function of temperature. From Eq. (1), we observe that the velocity component v is constant i.e. $v = v_0$.

The boundary conditions are given by

$$u = 0, \quad w = 0, \qquad \text{at} \quad y = \pm d, \tag{5a}$$

$$u_{yy} = 0, \quad w_{yy} = 0, \quad \text{at} \quad y = \pm d, \tag{5b}$$

$$T = T_1, \quad \text{at} \quad y = -d, \quad T = T_2, \quad \text{at} \quad y = d. \tag{5c}$$

The boundary condition equation (5a) corresponds to the classical no-slip condition from viscous fluid dynamics. The boundary condition equation (5b) imply that the couple stresses are zero at the plate surfaces.

Introducing the following similarity transformations

$$y = \eta d, \qquad u = \frac{K_f}{\rho g\beta_T d^2}U, \qquad w = \frac{K_f}{\rho g\beta_T d^2}W, \qquad T - T_0 = \frac{K_f\mu}{\rho^2 g^2\beta_T^2 d^4}\theta, \tag{6}$$

in Eqs. (2)–(4), we get the following nonlinear system of differential equations

$$\alpha^2 U^{(iv)} - U'' + ReU' - \theta + \frac{Ha^2}{\alpha_e^2+\beta_h^2}(\alpha_e U + \beta_h W) = 0, \tag{7}$$

$$\alpha^2 W^{(iv)} - W'' + ReW' - \frac{Ha^2}{\alpha_e^2+\beta_h^2}(\beta_h U - \alpha_e W) = 0, \tag{8}$$

$$\theta'' - RePr\theta' + 2[(U')^2 + (W')^2] + \alpha^2[(U'')^2 + (W'')^2] + \gamma_1 RePr\theta = 0, \tag{9}$$

where primes denote differentiation with respect to η, $\alpha = \sqrt{\eta_1/\mu}/d$ is the couple stress parameter, $Re = \rho v_0 d/\mu$ is the Reynolds number, $Pr = \mu C_p/K_f$ is the Prandtl number, $Ha = B_0 d\sqrt{\sigma/\mu}$ is the Hartmann number, $\gamma_1 = \gamma_0 d/\rho C_p$ is the dimensionless vertical distance and $Gr = g\beta_T d^3(T_1 - T_0)/\nu^2$ is the Grashof number. The effects of couple-stress are significant for large values of $\alpha(= l/d)$, where $l = \sqrt{\eta_1/\mu}$ is a material constant. If l is a function of molecular dimensions of the liquid, it will vary greatly for different liquids. For example, the length of a polymer chain may be a million times the diameter of water molecule [12]. Therefore, there are all the reasons to expect that couple-stresses appear in noticeable magnitudes in liquids with large molecules.

Boundary conditions equation (5) in terms of U, W, θ become

$$\begin{aligned} &U = 0, \quad W = 0, \quad U'' = 0, \\ &W'' = 0, \quad \theta = Q, \quad \text{at } \eta = -1, \\ &U = 0, \quad W = 0, \quad U'' = 0, \\ &W'' = 0, \quad \theta = \epsilon Q, \quad \text{at } \eta = 1, \end{aligned} \tag{10}$$

where $Q = PrGr\beta_T gd/C_p$ and $\epsilon = (T_2 - T_0)/(T_1 - T_0)$, the non-dimensional heating parameter

3 The HAM solution of the problem

For HAM solutions, we choose the initial approximations of $U(\eta)$, $W(\eta)$ and $\theta(\eta)$ as follows

$$U_0(\eta) = 0, \qquad W_0(\eta) = 0, \qquad \theta_0(\eta) = \frac{1}{2}(Q + \epsilon Q) + \frac{1}{2}(\epsilon Q - Q)\eta, \tag{11}$$

and choose the auxiliary linear operators

$$L_1 = \frac{\partial^4}{\partial\eta^4}, \quad L_2 = \frac{\partial^2}{\partial\eta^2}, \tag{12}$$

such that

$$L_1(c_1 + c_2\eta + c_3\eta^2 + c_4\eta^3) = 0, \qquad L_2(c_5 + c_6\eta) = 0, \tag{13}$$

where c_i $(i = 1, 2, \cdots, 6)$ are constants. Introducing non-zero auxiliary parameters h_1, h_2 and h_3, we develop the zeroth-order deformation problems as

$$(1 - p)L_1[U(\eta; p) - U_0(\eta)] = ph_1 N_1[U(\eta; p)], \tag{14}$$

$$(1 - p)L_1[W(\eta; p) - W_0(\eta)] = ph_2 N_2[W(\eta; p)], \tag{15}$$

$$(1-p)L_2[\theta(\eta;p)-\theta_0(\eta)] = ph_3N_3[\theta(\eta;p)], \tag{16}$$

subject to the boundary conditions of

$$\begin{aligned} &U(-1;p)=0, && U(1;p)=0,\\ &U''(-1;p)=0, && U''(1;p)=0,\\ &W(-1;p)=0, && W(1;p)=0,\\ &W''(-1;p)=0, && W''(1;p)=0,\\ &\theta(-1;p)=Q, && \theta(1;p)=\epsilon Q, \end{aligned} \tag{17}$$

where $p \in [0,1]$ is the embedding parameter and non-linear operators N_1, N_2 and N_3 are defined as

$$\begin{aligned} &N_1[U(\eta,p),W(\eta,p),\theta(\eta,p)]\\ &\quad = \alpha^2U^{(iv)}(\eta,p) - U''(\eta,p) + ReU'(\eta,p)\\ &\qquad -\theta(\eta,p) + \frac{Ha^2}{\alpha_e^2+\beta_h^2}(\alpha_eU+\beta_hW), \end{aligned} \tag{18}$$

$$\begin{aligned} &N_2[U(\eta,p),W(\eta,p),\theta(\eta,p)]\\ &\quad = \alpha^2W^{(iv)}(\eta,p) - W''(\eta,p) + ReW'(\eta,p)\\ &\qquad -\frac{Ha^2}{\alpha_e^2+\beta_h^2}(\beta_hU-\alpha_eW), \end{aligned} \tag{19}$$

$$\begin{aligned} &N_3[U(\eta,p),W(\eta,p),\theta(\eta,p)]\\ &\quad = \theta''(\eta,p) - RePr\theta'(\eta,p)\\ &\qquad +\gamma_1RePr\theta + 2[(U'(\eta,p))^2 + (W'(\eta,p))^2]\\ &\qquad +\alpha^2[(U''(\eta,p))^2 + (W''(\eta,p))^2]. \end{aligned} \tag{20}$$

For $p = 0$ we have the initial guess approximations

$$U(\eta;0) = U_0(\eta), \quad W(\eta;0) = W_0(\eta), \quad \theta(\eta;0) = \theta_0(\eta). \tag{21}$$

When $p = 1$, Eqs. (14)–(16) are the same as Eqs. (7)–(9), respectively, therefore at $p = 1$ we get the final solutions

$$U(\eta;1) = U(\eta), \quad W(\eta;1) = W(\eta), \quad \theta(\eta;1) = \theta(\eta). \tag{22}$$

Hence the process of giving an increment to p from 0 to 1 is the process of $U(\eta;p)$ varying continuously from the initial guess $U_0(\eta)$ to the final solution $U(\eta)$ (similar for $W(\eta,p)$ and $\theta(\eta,p)$). This kind of continuous variation is called deformation in topology so that we call system Eqs. (14)–(17), the zeroth-order deformation equation. Next, the m-th-order deformation equations follow as

$$L_1[U_m(\eta) - \chi_mU_{m-1}(\eta)] = h_1R_m^U(\eta), \tag{23}$$

$$L_1[W_m(\eta) - \chi_mW_{m-1}(\eta)] = h_2R_m^W(\eta), \tag{24}$$

$$L_2[\theta_m(\eta) - \chi_m\theta_{m-1}(\eta)] = h_3R_m^\theta(\eta), \tag{25}$$

with the boundary conditions of

$$\begin{aligned} &U_m(-1)=0, && U_m(1)=0,\\ &U_m''(-1)=0, && U_m''(1)=0,\\ &W_m(-1)=0, && W_m(1)=0,\\ &W_m''(-1)=0, && W_m''(1)=0,\\ &\theta_m(-1)=0, && \theta_m(1)=0, \end{aligned} \tag{26}$$

where

$$\begin{aligned} R_m^U(\eta) &= \alpha^2U^{(iv)} - U'' + ReU' - \theta\\ &\quad + \frac{Ha^2}{\alpha_e^2+\beta_h^2}(\alpha_eU+\beta_hW), \end{aligned} \tag{27}$$

$$\begin{aligned} R_m^W(\eta) &= \alpha^2W^{(iv)} - W'' + ReW'\\ &\quad - \frac{Ha^2}{\alpha_e^2+\beta_h^2}(\beta_hU-\alpha_eW), \end{aligned} \tag{28}$$

$$\begin{aligned} R_m^\theta(\eta) &= \theta'' - RePr\theta' + \gamma_1RePr\theta\\ &\quad +2\Big[\sum_{n=0}^{m-1}(U'_{m-1-n}U'_n + W'_{m-1-n}W'_n)\Big]\\ &\quad +\alpha^2\Big[\sum_{n=0}^{m-1}(U''_{m-1-n}U''_n + W''_{m-1-n}W''_n)\Big], \end{aligned} \tag{29}$$

for m being integer

$$\begin{aligned} &\chi_m = 0, && \text{for} \quad m \le 1,\\ &\chi_m = 1, && \text{for} \quad m > 1. \end{aligned} \tag{30}$$

The initial guess approximations $U_0(\eta)$, $W_0(\eta)$ and $\theta_0(\eta)$, the linear operators L_1, L_2 and the auxiliary parameters h_1, h_2 and h_3 are assumed to be so selected that Eqs. (14)–(17) have solution at each point $p \in [0,1]$. With the help of Taylors series and by referring to Eq. (21) $U(\eta;p)$, $W(\eta;p)$ and $\theta(\eta;p)$ can be expressed as

$$U(\eta;p) = U_0(\eta) + \sum_{m=1}^{\infty}U_m(\eta)p^m, \tag{31}$$

$$W(\eta;p) = W_0(\eta) + \sum_{m=1}^{\infty}W_m(\eta)p^m, \tag{32}$$

$$\theta(\eta;p) = \theta_0(\eta) + \sum_{m=1}^{\infty}\theta_m(\eta)p^m, \tag{33}$$

in which h_1, h_2 and h_3 are choosen in such a way that the series equations (31)–(33) are convergent [22] at $p = 1$. Therefore we have from Eq. (22) that

$$U(\eta) = U_0(\eta) + \sum_{m=1}^{\infty}U_m(\eta), \tag{34}$$

$$W(\eta) = W_0(\eta) + \sum_{m=1}^{\infty}W_m(\eta), \tag{35}$$

$$\theta(\eta) = \theta_0(\eta) + \sum_{m=1}^{\infty}\theta_m(\eta), \tag{36}$$

for which we presume that the initial guesses to U, W and θ the auxiliary linear operators L and the non-zero auxiliary parameters h_1, h_2 and h_3 are so properly selected that the deformation $U(\eta, p)$, $W(\eta, p)$ and $\theta(\eta, p)$ are smooth enough and their m-th-order derivatives with respect to p in Eqs. (34)–(36) exist and are given, respectively, by $U_m(\eta) = \frac{1}{m!}\frac{\partial^m U(\eta;p)}{\partial p^m}\Big|_{p=0}$, $W_m(\eta) = \frac{1}{m!}\frac{\partial^m W(\eta;p)}{\partial p^m}\Big|_{p=0}$, $\theta_m(\eta) = \frac{1}{m!}\frac{\partial^m \theta(\eta;p)}{\partial p^m}\Big|_{p=0}$. It is clear that the convergence of Taylor series at $p = 1$ is a prior assumption, whose justification is provided via a theorem [21], so that the system in Eqs. (34)–(36) holds true. The formulae in Eqs. (34)–(36) provide us a direct relationship between the initial guesses and the exact solutions. All the effects of interaction of the magnetic field as well as of the heat transfer, Hall and Ion effects and couple stress flow field can be studied from the exact formulas (34)–(36). Moreover, a special emphasize should be placed here that the m-th-order deformation system (23)–(26) is a linear differential equation system with an auxiliary linear operators L whose fundamental solution is known.

4 Convergence of the HAM solution

The expressions for U, W and θ contain the auxiliary parameters h_1, h_2 and h_3. As pointed out by Liao [15], the convergence and the rate of approximation for the HAM solution depend strongly on the values of auxiliary parameter h. For this purpose, h-curves are plotted by choosing h_1, h_2 and h_3 in such a manner that the solutions (31)–(33) ensure convergence [15]. Here to see the admissible values of h_1, h_2 and h_3, the h-curves are plotted for 15th-order of approximation in Figs. 2–4 by taking the values of the parameters as: $Pr = 0.71$, $Q = 1$, $\epsilon = 0.5$, $\gamma_1 = 1$, $Re = 2$, $\beta_h = 2$, $\beta_i = 2$, $\alpha = 0.5$ and $Ha = 5$. It is clearly noted from Fig. 2 that the range for the admissible values of h_1 is $-1.25 < h_1 < -0.75$. From Fig. 3, it can be seen that the h-curve has a parallel line segment that corresponds to a region of $-1.25 < h_2 < -0.75$. Figure 4 depicts that the admissible value of h_3 are $-1.5 < h_3 < -0.5$. A wide valid zone is evident in these figures ensuring convergence of the series. To choose optimal value of the auxiliary parameter, the average residual errors (see Ref. [17] for more details) are defined as

$$E_{U,m} = \frac{1}{2K}\sum_{i=-K}^{K}\left\{N_1\Big[\sum_{j=0}^{m} U_j(i\Delta t)\Big]\right\}^2, \tag{37}$$

$$E_{W,m} = \frac{1}{2K}\sum_{i=-K}^{K}\left\{N_2\Big[\sum_{j=0}^{m} W_j(i\Delta t)\Big]\right\}^2, \tag{38}$$

$$E_{\theta,m} = \frac{1}{2K}\sum_{i=-K}^{K}\left\{N_3\Big[\sum_{j=0}^{m} \theta_j(i\Delta t)\Big]\right\}^2, \tag{39}$$

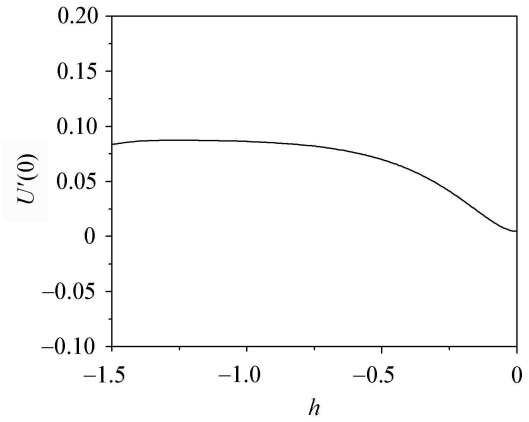

Fig. 2 The h curve of $U(\eta)$ when $\beta_h = 2, \beta_i = 2, \alpha = 0.5, Ha = 5$

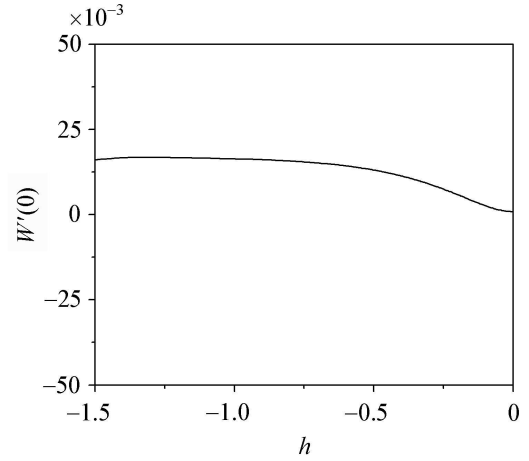

Fig. 3 The h curve of $W(\eta)$ when $\beta_h = 2, \beta_i = 2, \alpha = 0.5, Ha = 5$

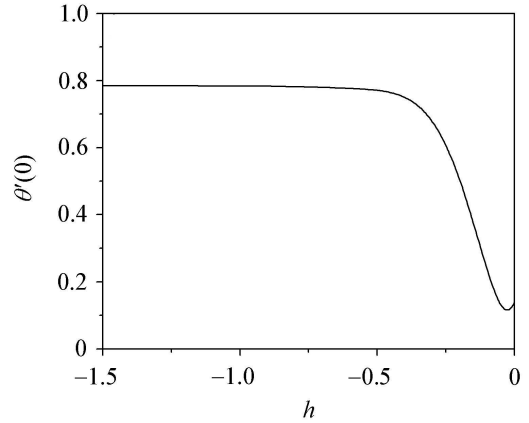

Fig. 4 The h curve of $\theta(\eta)$ when $\beta_h = 2, \beta_i = 2, \alpha = 0.5, Ha = 5$

where $\Delta t = 1/K$ and $K = 5$. At different orders of approximations (m), the minimum of average residual errors are shown in Tables 1–3. It is clear from Table 1 that the average residual error for U is minimum at $h_1 = -1.04$. It

can be seen from Table 2 that the minimum of average residual error for W attains $h_2 = -0.98$. Table 3 depicts that at $h_3 = -1.025$, E_θ attains minimum. Therefore, the optimum values of convergence control parameters are taken as $h_1 = -1.04$, $h_2 = -0.98$, $h_3 = -1.025$.

Table 1 Optimal value of h_1 at different orders of approximations

Order	Optimal of h_1	Minimum of E_m
10	−1.04	1.19×10^{-5}
15	−1.04	4.16×10^{-6}
20	−1.04	2.41×10^{-7}

Table 2 Optimal value of h_2 at different orders of approximations

Order	Optimal of h_2	Minimum of E_m
10	−0.94	1.77×10^{-7}
15	−0.98	5.15×10^{-8}
20	−0.98	2.72×10^{-8}

Table 3 Optimal value of h_3 at different orders of approximations

Order	Optimal of h_3	Minimum of E_m
10	−1.020	7.82×10^{-5}
15	−1.025	8.92×10^{-6}
20	−1.025	8.84×10^{-7}

To see the accuracy of the solutions, the residual errors are defined for the system as

$$RE_U = \alpha^2 U_n^{(iv)}(\eta) - U_n''(\eta) + ReU_n'(\eta) - \theta_n(\eta) + \frac{Ha^2}{\alpha_\mathrm{e}^2 + \beta_\mathrm{h}^2}(\alpha_\mathrm{e} U_n + \beta_\mathrm{h} W_n), \tag{40}$$

$$RE_W = \alpha^2 W_n^{(iv)}(\eta) - W_n''(\eta) + ReW_n'(\eta) - \frac{Ha^2}{\alpha_\mathrm{e}^2 + \beta_\mathrm{h}^2}(\beta_\mathrm{h} U_n - \alpha_\mathrm{e} W_n), \tag{41}$$

$$RE_\theta = \theta_n''(\eta) - RePr\theta_n'(\eta) + \gamma_1 RePr\theta_n + 2[(U_n'(\eta))^2 + (W_n'(\eta))^2] + \alpha^2[(U_n''(\eta))^2 + (W_n''(\eta))^2], \tag{42}$$

where $U_n(\eta)$, $W_n(\eta)$ and $\theta_n(\eta)$ are the HAM solution for $U(\eta)$, $W(\eta)$ and $\theta(\eta)$. For optimizing the convergence control parameters, residual errors [18] for different values of h in the convergence region displayed in Figs. 5–7. We can see that $h_1 = -1.04$, $h_2 = -0.98$, $h_3 = -1.025$ gives a better solution. Table 4 establishes the convergence of the obtained series solution. It is found from the above observations that the series given by Eqs. (31)–(33) converge in the whole region of η when $h_1 = -1.04$, $h_2 = -0.98$, $h_3 = -1.025$.

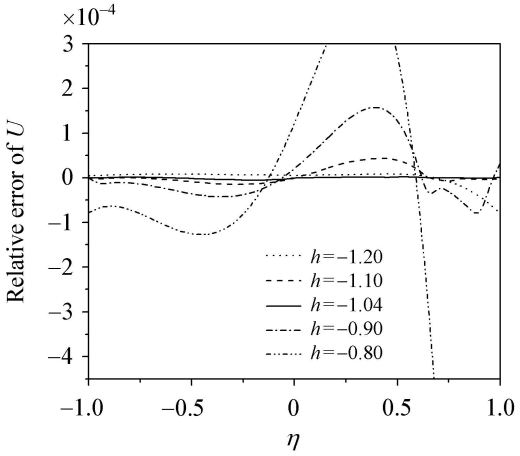

Fig. 5 Relative error of $U(\eta)$ when $\beta_\mathrm{h} = 2, \beta_\mathrm{i} = 2, \alpha = 0.5, Ha = 5$

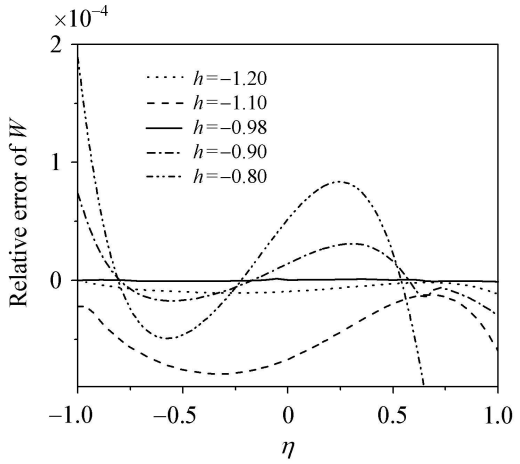

Fig. 6 Relative error of $W(\eta)$ when $\beta_\mathrm{h} = 2, \beta_\mathrm{i} = 2, \alpha = 0.5, Ha = 5$

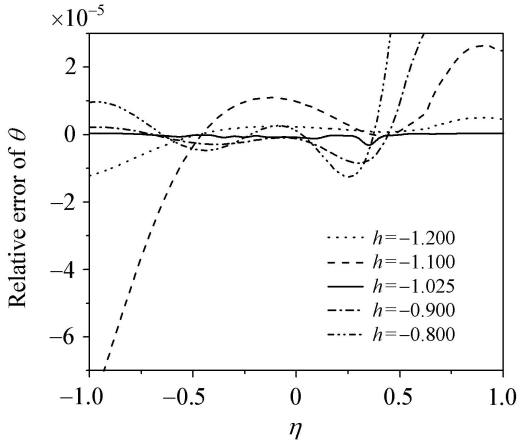

Fig. 7 Relative error of $\theta(\eta)$ when $\beta_\mathrm{h} = 2, \beta_\mathrm{i} = 2, \alpha = 0.5, Ha = 5$

In order to pursue the convergence of the HAM solutions to the exact ones, the graphs for the ratio (following the recent work of Ref. [21])

$$\beta_U = \left|\frac{U_m(h)}{U_{m-1}(h)}\right|,$$
$$\beta_W = \left|\frac{W_m(h)}{W_{m-1}(h)}\right|, \quad (43)$$
$$\beta_\theta = \left|\frac{\theta_m(h)}{\theta_{m-1}(h)}\right|,$$

against the number of terms m in the homotopy series is presented in Figs. 8–10. Figures strongly indicate that a finite limit of β will be attained in the limit of $m \to \infty$, which will remain less than unity (actually figures imply a limit of 0.91 for U, W and θ). The velocity and temperature solutions seem to converge in an oscillatory manner which requires more terms in the homotopy series. Thus, the convergence to the exact solution is assured by the HAM.

Table 4 Convergence of HAM solutions for different orders of approximations

Order	$U(0)$	$W(0)$	$\theta(0)$
1	0.256 250 000 0	0	1.860 000 000
5	0.266 892 314 4	0.055 651 358 0	2.113 014 591
10	0.268 922 610 6	0.054 909 169 1	2.137 602 471
15	0.268 624 370 8	0.054 728 226 6	2.138 233 341
20	0.268 624 361 9	0.054 728 217 9	2.138 233 185
30	0.268 624 348 5	0.054 728 212 1	2.138 233 071
40	0.268 624 342 7	0.054 728 211 6	2.138 233 028
50	0.268 624 342 6	0.054 728 211 5	2.138 233 027

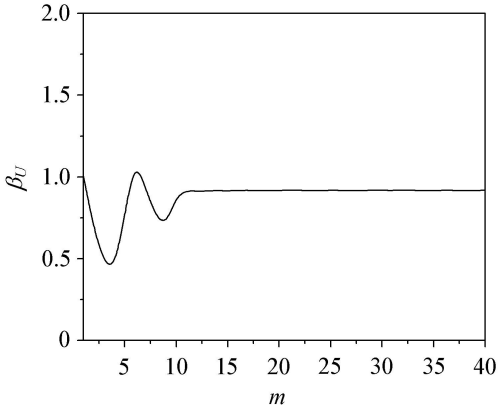

Fig. 8 The ratio β_U from the theorem to reveal the convergence of the HAM solutions

5 Results and discussion

The solutions for $U(\eta)$, $W(\eta)$ and $\theta(\eta)$ have been computed and shown graphically in Figs. 11 to 22. The effects of magnetic parameter (Ha), Hall parameter (β_h), ion-slip parameter (β_i) and couple stress fluid parameter (α) have been discussed. To study the effect of Ha, β_h, β_i and α, computations were carried out by taking $Pr = 0.71$, $Q = 1$, $\epsilon = 0.5$, $\gamma_1 = 1$, $Re = 2$ and $h_1 = -1.04$, $h_2 = -0.98$, $h_3 = -1.025$.

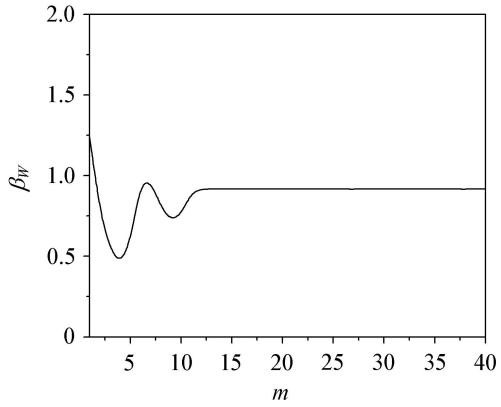

Fig. 9 The ratio β_W from the theorem to reveal the convergence of the HAM solutions

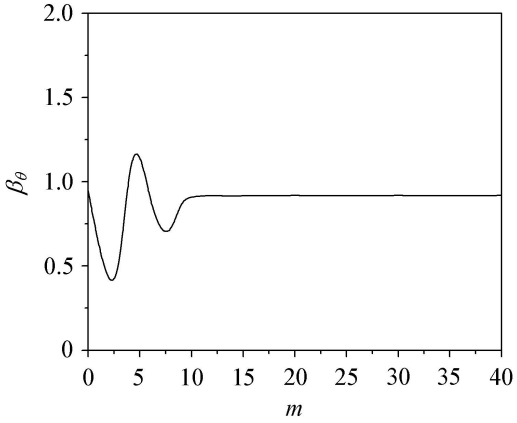

Fig. 10 The ratio β_θ from the theorem to reveal the convergence of the HAM solutions

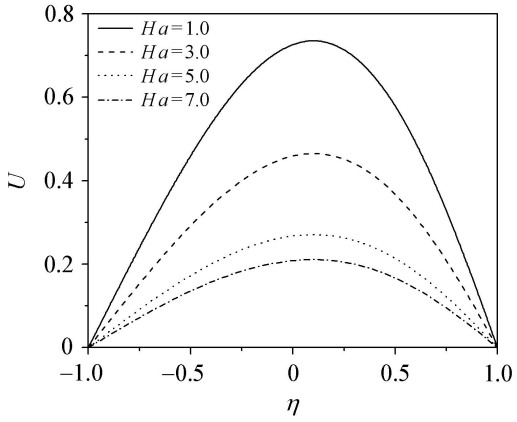

Fig. 11 The influence of the magnetic parameter Ha on U when $\beta_h = 2.0$, $\beta_i = 2.0$, $\alpha = 0.5$

Figure 11 displays the effect of the magnetic parameter Ha on $U(\eta)$. It can be observed that the velocity $U(\eta)$ decreases with an increase in parameter Ha. This is due to the fact that, the introduction of a transverse magnetic field, normal to the flow direction, has a tendency to create the drag known as the Lorentz force which tends to resist the flow. Hence the velocity decrease as the magnetic parame-

ter Ha increases. The effect of Ha on the induced flow in z-direction $W(\eta)$ is shown in Fig. 12. It can be seen from this figure that $W(\eta)$ increases with an increase in parameter Ha. Figure 13 depicts the variation of temperature with Ha. The temperature $\theta(\eta)$ decreases with an increase in parameter Ha. As explained above, the transverse magnetic field gives rise to a resistive force known as the Lorentz force of an electrically conducting fluid. This force makes the fluid experience a resistance by increasing the friction between its layers and thus decreases its temperature and concentration.

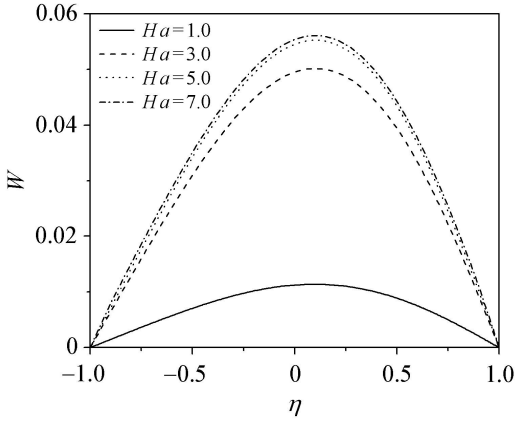

Fig. 12 The influence of the magnetic parameter Ha on W when $\beta_h = 2.0, \beta_i = 2.0, \alpha = 0.5$

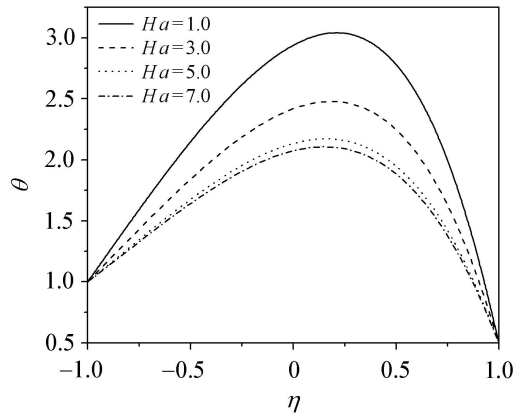

Fig. 13 The influence of the magnetic parameter Ha on θ when $\beta_h = 2.0, \beta_i = 2.0, \alpha = 0.5$

The variation of velocity components $U(\eta)$ and $W(\eta)$ and temperature $\theta(\eta)$ with β_h is shown in Figs. 14 to 16. We see that the dimensionless velocity component $U(\eta)$ and temperature $\theta(\eta)$ increase with an increase in parameter β_h. The inclusion of Hall parameter decreases the resistive force imposed by the magnetic field due to its effect in reducing the effective conductivity. Hence, the velocity component $U(\eta)$ and temperature $\theta(\eta)$ increases as the Hall parameter increases. The induced flow in the z-direction decreases as β_h increases.

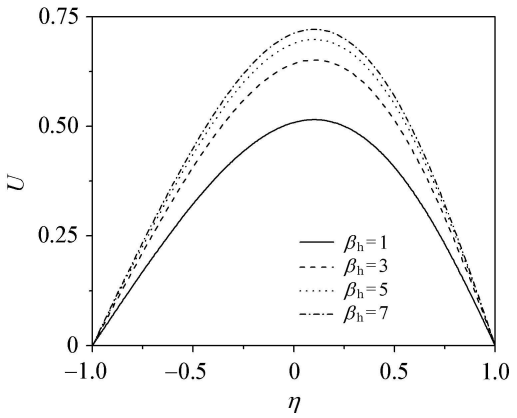

Fig. 14 The influence of the Hall parameter β_h on U when $\beta_i = 2.0$, $\alpha = 0.5$, $Ha = 2$

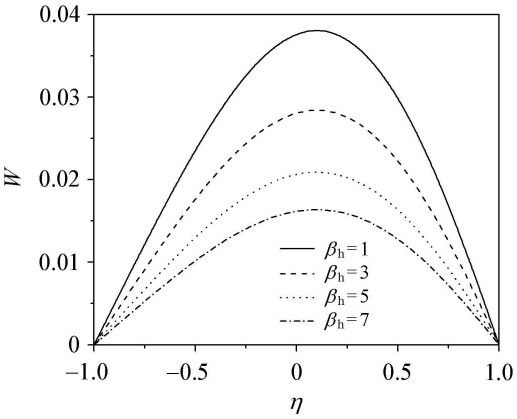

Fig. 15 The influence of the Hall parameter β_h on W when $\beta_i = 2.0$, $\alpha = 0.5$, $Ha = 2$

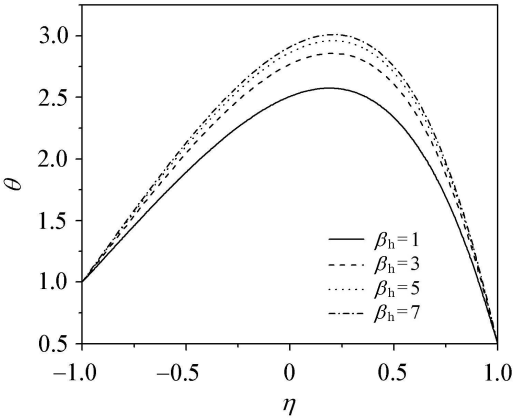

Fig. 16 The influence of the Hall parameter β_h on θ when $\beta_i = 2.0$, $\alpha = 0.5$, $Ha = 2$

Figures 17 to 19 represent the effect of the ion-slip parameter β_i on $U(\eta)$, $W(\eta)$ and $\theta(\eta)$. It can be seen from these figures that the velocity $U(\eta)$ increase with an increase in parameter β_i. The induced flow in the z-direction decreases with an increase in parameter β_i. The temperature $\theta(\eta)$ in-

creases with an increase in parameter β_i. As β_i increases the effective conductivity also increases, which in turn decreases the damping force on the velocity component in the direction of the flow, and hence the velocity component in the flow direction increases.

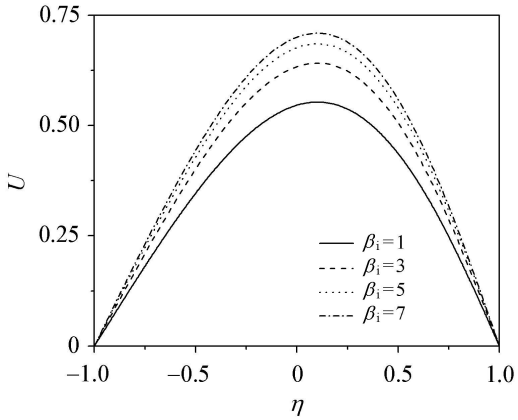

Fig. 17 The influence of the ion-slip parameter β_i on U when $\beta_h = 2.0$, $\alpha = 0.5$, $Ha = 2$

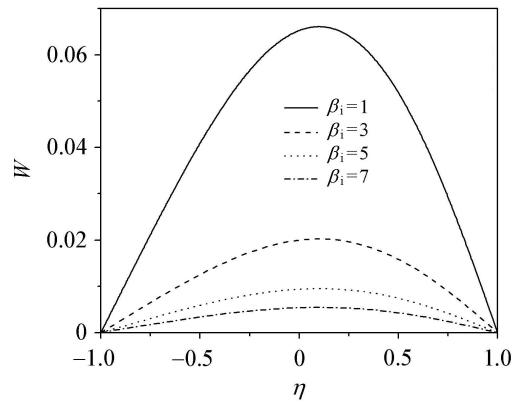

Fig. 18 The influence of the ion-slip parameter β_i on W when $\beta_h = 2.0$, $\alpha = 0.5$, $Ha = 2$

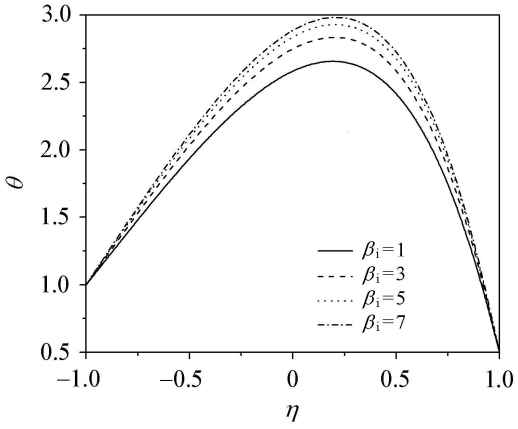

Fig. 19 The influence of the ion-slip parameter β_i on θ when $\beta_h = 2.0$, $\alpha = 0.5$, $Ha = 2$

Figures 20 to 22 indicate the effect of the couple stress fluid parameter α on $U(\eta)$, $W(\eta)$ and $\theta(\eta)$. As the couple stress fluid parameter α increases, the velocity $U(\eta)$, the induced flow in the z-direction $W(\eta)$ decrease. It is also clear

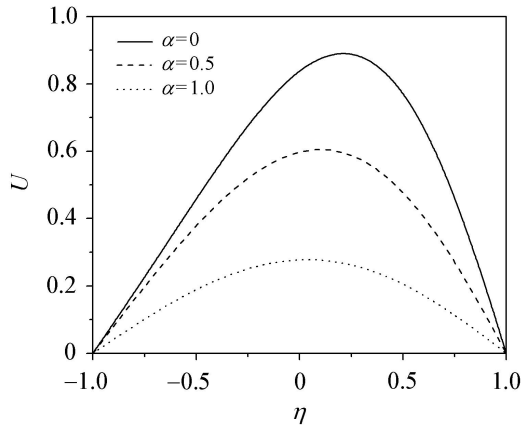

Fig. 20 The influence of the couple stress parameter (α) on U when $\beta_h = 2.0$, $\beta_i = 2.0$, $Ha = 2$

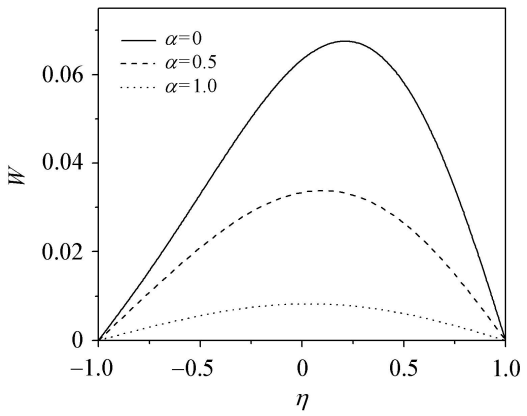

Fig. 21 The influence of the couple stress parameter (α) on W when $\beta_h = 2.0$, $\beta_i = 2.0$, $Ha = 2$

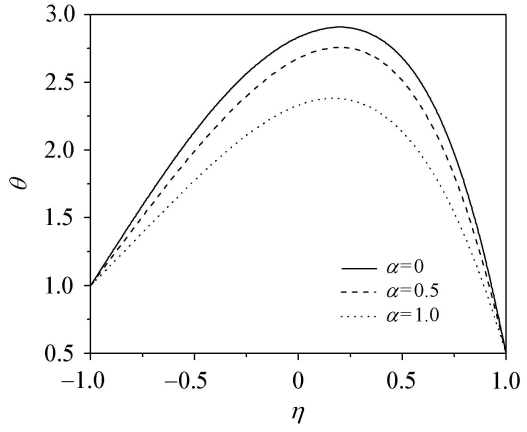

Fig. 22 The influence of the couple stress parameter (α) on θ when $\beta_h = 2.0$, $\beta_i = 2.0$, $Ha = 2$

that the temperature $\theta(\eta)$ decreases with an increase in α. It can be noted that the velocity in the case of couple stress fluid is less than that in the Newtonian fluid case. Thus, the presence of couple stresses in the fluid decreases the velocity and temperature.

6 Conclusions

In this paper, the Hall and ion-slip effects on fully developed electrically conducting couple stress fluid flow between vertical parallel plates has been studied. Using similarity transformations, the governing equations have been transformed into non-linear ordinary differential equations. The governing equations are expressed in the non-dimensional form and are then solved by HAM. The features of flow characteristics are analyzed by plotting graphs with detailed discussions. The main findings are summarized as follows:

(1) As the magnetic parameter increases, velocity in the direction of the flow and the temperature are decreased and the induced flow velocity component is increased.
(2) The velocity in the flow direction and temperature are increased and the induced flow in the *z*-direction is decreased as the Hall parameter increases.
(3) The velocity in the flow direction and the temperature increase and the induced flow in the *z*-direction decreases with an increase in the ion-slip parameter.
(4) It is noticed that the presence of couple stresses in the fluid decreases the velocity and temperature.

References

1 Elenbaas, W.: Heat dissipation of parallel plates by free convection. Physica, Col. **IX**(1), 1–7 (1942)
2 Bodoia, J.R., Osterle, J.F.: The development of free convection between heated vertical plates. ASME Journal of Heat Transfer **84**(1), 40–44 (1962)
3 Aung, W., Fletcher L.S., Sernas, V.: Developing laminar free convection between vertical flat plates with asymmetric heating. Int. J. Heat Mass Trasfer **15**, 2293–2308 (1972)
4 Singh, M.K.: MHD free convective flow through a porous medium between two vertical parallel plates. Indian Journal of Pure & Applied Physics **40**(10), 709–713 (2002)
5 Singha, K.G., Deka, P.K.: Skin-friction for unsteady free convection MHD flow between two heated vertical parallel plates. Theoret. Appl. Mech. **33**(4), 259–280 (2006)
6 Omowaye, A.J., Koriko, O.K.: Similarity solutions for free convection between two parallel porous walls at different temperatures. Journal of Mathematics and Statistics **6**(2), 143–150 (2010)
7 Tani, I.: Steady flow of conducting fluids in channels under transverse magnetic fields with consideration of Hall effects. J. of Aerospace Sci. **29**, 297–305 (1962)
8 Sondalgekar, V.M., Vighnesam, N.V., Takhar, H.S.: Hall and ion-slip effects in MHD Couette flow with heat trasfer. IEEE Transactions of Plasma Sci. **7**, 178–182 (1979)
9 Attia, H.A.: Unsteady couette flow with heat transfer considering ion-slip. Turk J. Phys. **29**, 379–388 (2005)
10 Ziabakhsh, Z., Domairry, G.: Analytic solution of natural convection flow of a non-Newtonian fluid between two vertical flat plates using homotopy analysis method. Commun. Nonlinear Sci. Numer. Simulat. **14**, 1868–1880 (2009)
11 Sajid, M., Pop, I., Hayat, T.: Fully developed mixed convection flow of a viscoelastic fluid between permeable parallel vertical plates. Computers and Mathematics with Applications **59**, 493–498 (2010)
12 Stokes, V. K.: Couple stresses in fluid. The Physics of Fluids **9**(9), 1709–1715 (1966)
13 Stokes, V. K.: Theories of Fluids with Microstructure: An Introduction. Springer Verlag, New York (1984)
14 Srinivasacharya, D., Srikanth, D.: Effect of couple stresses on the flow in a constricted annulus. Arch. Appl. Mech. **78**, 251–257 (2008) doi 10.1007/s00419-007-0157-6
15 Liao, S.J.: Beyond Perturbation. Introduction to Homotopy Analysis Method. Chapman and Hall/CRC Press, and Boca Raton (2003)
16 Liao, S.J.: On the homotopy analysis method for nonlinear problems. Appl. Math. Comput. **147**(2), 499–513 (2004)
17 Liao, S.J.: An optimal homotopy-analysis approach for strongly nonlinear differential equations. Commun. Nonlinear Sci. Numer. Simulat. **15**, 2003–2016 (2010)
18 Rashidi, M.M., Mohimanian pour, S.A., Abbasbandy, S.: Analytic approximate solutions for heat transfer of a micropolar fluid through a porous medium with radiation. Commun. Nonlinear Sci. Numer. Simulat. **16**, 1874–1889 (2011)
19 Si, X.-H., Zheng, L.-C., Zhang, X.-X., et al.: Homotopy analysis solutions for the asymmetric laminar flow in a porous channel with expanding or contracting walls. Acta Mech. Sin. **27**(2), 208–214 (2011)
20 Turkyilmazoglu, M.: Some issues on HPM and HAM methods: A convergence scheme. Mathematical and Computer Modelling **53**, 1929–1936 (2011)
21 Turkyilmazoglu, M.: Numerical and analytical solutions for the flow and heat transfer near the equator of an MHD boundary layer over a porous rotating sphere. International Journal of Thermal Sciences **50**, 831–842 (2011)
22 Liao, S.J.: On the relationship between the homotopy analysis method and Euler transform. Commun. Nonlinear Sci. Numer. Simul. **14**, 1421–1431 (2010)